2001

Data Report: Carbon Isotopic Composition of Dissolved CO2, CO2 Gas, and Methane, Blake-Bahama Ridge and Northeast Bermuda Rise, ODP Leg 172

Walter S. Borowski
Eastern Kentucky University, w.borowski@eku.edu

Namik Cagatay

Y Tournois

Charles K. Paull
MBARI

Recommended Citation

Borowski, W.S., N. Cagatay, Y. Tournois, C.K. Paull. 2001. Data report: Carbon isotopic composition of dissolved CO2, CO2 gas, and methane, Blake-Bahama Ridge and northeast Bermuda Rise, ODP Leg 172. In L.D. Keigwin, D. Rio, G.D. Acton, and E. Arnold (Eds.), 2001, Proceedings ODP, Scientific Results, 172.

Keigwin, L.D., Rio, D., Acton, G.D., and Arnold, E. (Eds.)
Proceedings of the Ocean Drilling Program, Scientific Results Volume 172

3. Data Report: Carbon Isotopic Composition of Dissolved CO_2, CO_2 Gas, and Methane, Blake-Bahama Ridge and Northeast Bermuda Rise, ODP Leg 172[1]

Walter S. Borowski,[2,3] Namik Cagatay,[4] Yann Ternois,[5] and Charles K. Paull[2,6]

ABSTRACT

Carbon isotopic data of interstitial dissolved CO_2 (ΣCO_2), CO_2 gas, and methane show that a variety of microbial diagenetic processes produce the observed isotopic trends. Anaerobic methane oxidation (AMO) is an important process near the sulfate-methane interface (SMI) that strongly influences the isotopic composition of ΣCO_2 in the sulfate reduction and upper methanogenic zones, which in turn impacts methane isotopic composition. Dissolved CO_2 and methane are maximally depleted in ^{13}C near the SMI, where $\delta^{13}C$ values are as light as –31.8‰ and –101‰ PDB for ΣCO_2 and methane, respectively. CO_2 reduction links the CO_2 and methane pools in the methanogenic zone so that the carbon isotopic composition of both pools evolves in concert, generally showing increasing enrichments of ^{13}C with increasing depth. These isotopic trends mirror those within other methane-rich continental rise sediments worldwide.

INTRODUCTION

Early diagenetic processes occurring in the pore waters of deep-water, continental-margin sediments are typically mediated by microbial pop-

[1]Borowski, W.S., Cagatay, N., Ternois, Y., and Paull, C.K., 2000. Data report: Carbon isotopic composition of dissolved CO_2, CO_2 gas, and methane, Blake-Bahama Ridge and northeast Bermuda Rise, ODP Leg 172. *In* Keigwin, L.D., Rio, D., Acton, G.D., and Arnold, E. (Eds.), *Proc. ODP, Sci. Results,* 172, 1–16 [Online]. Available from World Wide Web: <http://www-odp.tamu.edu/publications/172_SR/VOLUME/CHAPTERS/SR172_03.PDF>. [Cited YYYY-MM-DD]
[2]Department of Geological Sciences, University of North Carolina, Chapel Hill NC 27599-3315, USA.
[3]Present address: Department of Geology and Geography, DePauw University, Greencastle IN 46135, USA. **borowski@lcc.net**
[4]Department of Geology, School of Mines, Istanbul Technical University, Maslak, Istanbul 80626, Turkey
[5]Centre des Faibles Radioactivies (CFR) (UPR 2101) CNRS, Avenue de la Terrasse, 91191 Gif-sur-yvette Cedex, France
[6]Monterey Bay Aquarium Research Institute, PO Box 628, Moss Landing CA 95039-0628, USA.

Initial receipt: 19 August 1999
Acceptance: 21 March 2000
Web publication: 12 October 2000
Ms 172SR-201

ulations. Microbes use various dissolved species to oxidize sedimentary organic matter resulting in modification of the concentration and isotopic composition of dissolved pore-water constituents by removing needed substrates, adding metabolic by-products, and creating a reactive chemical environment (e.g., Richards, 1965; Gieskes, 1981). Carbon transformations particularly reveal these fundamental processes, as organic carbon from sedimentary organic matter is ultimately transformed into CO_2 and methane, passing through a cascade of intermediate steps (generally called fermentation reactions).

Terminal carbon transformations of methane-rich diagenetic environments of the world's deep-water continental margins involve several diagenetic processes that are linked by common substrates and/or products. Sulfate reducers utilize interstitial sulfate to oxidize sedimentary organic matter and produce CO_2, which dominantly exists in marine pore waters as bicarbonate (HCO_3^-). Deeper in the sedimentary section, anaerobic methane oxidation and methanogenesis occur to further affect the concentration and isotopic composition of dissolved CO_2 (ΣCO_2 or dissolved inorganic carbon) and methane.

Anaerobic Methane Oxidation

At the base of the sulfate reduction zone, microbially mediated anaerobic methane oxidation (AMO),

$$CH_4 + SO_4^{2-} \rightarrow HCO_3^- + HS^- + H_2O,$$

acting near the sulfate-methane interface (SMI), causes both sulfate and methane depletion (Reeburgh, 1976). Deep-water marine sediments on continental margins often show linear sulfate profiles, suggestive of large amounts of sulfate consumption at the SMI caused by AMO (Borowski et al., 1996). Borowski et al. (2000) estimate that at least 35% of interstitial sulfate is consumed by AMO in such settings, highlighting a significant role for AMO in deep-water diagenetic systems.

Carbon Cycling at the SMI

Carbon cycling is a demonstrably important process at the sulfate-methane interface and within the uppermost methanogenic zone of marine, deep-water continental margins. AMO strongly affects the carbon isotopic composition of the CO_2 and methane pools (Borowski et al., 1997) and also induces authigenic formation of carbonate minerals (e.g., Rodriguez et al., 2000). Borowski et al. (1997) showed that AMO, operating over long time spans in an open diagenetic system, induces extreme ^{13}C depletions in both the CO_2 and methane pools. For example, at the Blake Ridge, pore water ΣCO_2 can be as depleted in ^{13}C as –38‰ PDB (Ocean Drilling Program [ODP] Site 995, Borowski et al., 2000), signaling a large contribution of methane carbon to the CO_2 pool. Complementary ^{13}C depletions in the methane pool can be as large as –103‰ near the SMI (ODP Site 995, Hoehler et al., 2000). These large ^{13}C depletions near the SMI ripple downward into the underlying sedimentary section. ^{13}C depletions within ΣCO_2 and methane occur within the upper methanogenic zone as a consequence of downward diffusion, and because ^{13}C-depleted ΣCO_2 is used as a substrate in methanogenesis (Claypool and Kaplan, 1974; Borowski et al., 1997; Paull et al., 2000).

Methanogenesis

Once pore-water sulfate nears depletion in marine sediments, microbially mediated methane production is favored so that dissolved methane concentrations rise in pore waters (Martens and Berner, 1974). Geochemical data from the Blake Ridge, gathered from Deep Sea Drilling Project (DSDP) and ODP drilling, show a connection between the CO_2 and methane pools as methanogenesis occurs (e.g., Claypool and Kaplan, 1974; Claypool and Threlkeld, 1983; Galimov and Kvenvolden, 1983). CO_2 reduction,

$$CO_2 + 4H_2 \rightarrow CH_4 + H_2O,$$

is probably the principal mechanism for biotic methane formation in marine sediments (Whiticar et al., 1986), and the process links these two carbon pools within the methanogenic zone. The isotopic composition of interstitial methane and ΣCO_2 evolve in concert as ^{12}C is preferentially utilized from the ΣCO_2 pool for methane formation, causing the ΣCO_2 pool to become depleted in ^{12}C (yielding more positive, or heavy, $\delta^{13}C$ values), whereas the methane pool is immediately enriched in ^{12}C (yielding very negative, or light, $\delta^{13}C$ values), but progressively accumulates more ^{13}C with depth. However with increasing depth, the isotopic composition of ΣCO_2 and methane begin to diverge with ΣCO_2 becoming more enriched in ^{12}C, and methane showing little change in its $\delta^{13}C$ values (e.g., ODP Sites 994, 995, and 997, Borowski et al., 2000; Paull et al., 2000). In other words, the two carbon pools seem to decouple, suggesting a drop in the rate of CO_2 reduction, even though sediments are warming along a geothermal gradient (Paull et al., 2000).

Methane and CO_2 Advection

It is likely that a significant proportion of the interstitial methane in the deeper sedimentary section is derived not from in situ production but from methane and/or pore-water transport (Paull et al., 2000). Paull et al. (2000) suggest that upward transport of methane and CO_2 affects the carbon isotopic composition of both pools at the Blake Ridge. A model that uses a typical fractionation factor for CO_2 reduction ($\Sigma CO_2 \rightarrow CH_4$), that progressively decreases microbial methane production with depth, and that adds methane and CO_2 to the lower sedimentary section from deeper below, mimicked typical isotopic profiles seen at the Blake Ridge.

Blake Ridge

The Blake Ridge region has long been a favored area for geochemical investigations because of its relative geologic simplicity and the presence of gas hydrates (DSDP Leg 11, Sites 102, 103, and 104, Hollister, Ewing, et al., 1972; DSDP Leg 76, Site 533, Sheridan, Gradstein, et al., 1983; and ODP Leg 164, Sites 994, 995, and 997, Paull, Matsumoto, Wallace, et al., 1996) (Fig. F1). ODP Leg 172 continued investigations on the Blake Ridge (Sites 1054–1061) and included sites at the Bahama Ridge (Site 1062) and at the northeast Bermuda Rise (Site 1063) (Keigwin, Rio, Acton, et al., 1998).

Here we report ΣCO_2 concentrations and the carbon isotopic composition of ΣCO_2, CO_2 gas (derived as a small portion of the ΣCO_2 pool

F1. Map showing DSDP and ODP sites at the Carolina Rise, Blake Ridge, and Bahama Ridge, p. 10.

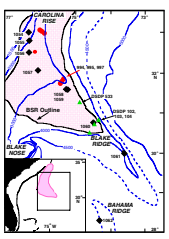

outgasses during sediment recovery), and methane from ODP Leg 172 to add to the global inventory of carbon isotope measurements.

METHODS

Sediments collected from ODP cores were sampled and processed using standard ODP methods, except that pore waters were sampled more frequently (approximately every 1.5 m) in the upper 50 m of the sedimentary section. Pore waters were extracted from sediments using a hydraulic sediment press (Manheim, 1966) and collected in air-tight syringes (Manheim and Sayles, 1974). At Site 1059, 60-cm^3 syringes attached to Reeburgh-style squeezers (Reeburgh, 1967) were used to collect pore waters and interstitial gases from selected samples. This method has the advantage of collecting interstitial gases for isotopic measurements. Sulfate concentration was determined by ion chromatography, and alkalinity was measured by titration (Gieskes et al., 1991). Methane concentrations were measured on board ship using headspace methods and employing a gas chromatograph fitted with a flame ionization detector (FID) (Kvenvolden and McDonald, 1985). Methane concentration measurements gathered using headspace methods were normalized to pore-space volume (e.g., Paull, Matsumoto, Wallace, et al., 1996). Pore-water aliquots for onshore ΣCO_2 measurements were stored immediately after squeezing in flame-sealed, air-tight ampoules.

Onshore, ΣCO_2 was separated and purified using cryogenic techniques (e.g., Craig, 1953). Carbon-isotopic-composition measurements of ΣCO_2 are reported relative to the Peedee belemnite (PDB) standard, and were made using a Delta E mass spectrometer at North Carolina State University. The cumulative (vacuum line and mass spectrometer) accuracy and precision of isotopic measurements are ±0.2‰ and ±0.06‰ (N. Blair, pers. comm., 1998).

Methane and CO_2 gases were typically collected directly from core liners using a piercing tool that directed pressured gas into a 60-cm^3 syringe (e.g., Paull, Matsumoto, Wallace, et al., 1996). Gas subsamples were taken from syringes, and gas composition and concentration was measured using a gas chromatograph fitted with an FID. Any remaining sample was transferred under water to 60-cm^3 serum bottles. In cases where there was insufficient sample to completely fill serum bottles, nitrogen gas was used to fill the bottles leaving only small amounts of water. Thus, contamination with ambient air was avoided. The bottles were sealed with rubber stoppers and metal crimp caps, inverted, and frozen for later measurement in an onshore laboratory.

Gas samples were stripped of their water onshore using cryogenic techniques (e.g., Craig, 1953). CO_2 and methane gas fractions were then separated and $\delta^{13}C$ of CO_2 gas and methane was measured using a Finnigan MAT 252 gas chromatograph-isotope ratio-mass spectrometer at the University of North Carolina at Chapel Hill following the methods of Merritt and Hayes (1995) and Popp et al. (1995).

Sediment coring during ODP advanced piston coring often results in repeated coring of the same portion of the sedimentary section or lack of sediment recovery over a portion of the sedimentary section within the same hole. Coring of multiple holes at each site allowed a composite stratigraphic section to be constructed that is reported as meters cor-

rected depth (mcd) below the sediment-water interface (see Keigwin, Rio, Acton, et al., 1998).

RESULTS

Tables T1 and T2 contain concentration and carbon isotopic data for the Carolina Rise (Sites 1054 and 1055), the Blake Ridge (Sites 1058–1061), the Bahama Ridge (Site 1062), and the northeast Bermuda Rise (Site 1063). Figure F2 shows representative concentration-depth profiles of sulfate, alkalinity, and ΣCO_2, and $\delta^{13}C$ of ΣCO_2 and methane at Sites 1058 and 1059, which were plotted as a single hole location and are referred to as Site 1058/1059. Figure F3 shows the carbon isotopic composition of ΣCO_2 and methane, with respect to the SMI, for all sites. Between the sites, the depth of the SMI varies between 10 and 67 mbsf (13 and 75 mcd); the order of increasing depth to SMI at 172 sites is 1058/1059, 1060, 1061, 1055, 1063, 1054, and 1062.

Dissolved CO_2

The carbon isotopic composition of the ΣCO_2 pool is most depleted in ^{13}C at the SMI at all sites, but the intensity of ^{13}C-depletion varies from site to site (Table T1). Starting at the sediment-water interface, ΣCO_2 becomes progressively enriched in ^{12}C with increasing depth into the sulfate reduction zone, reaching maximum ^{13}C depletion (^{12}C enrichment) at the SMI. Site 1058/1059 (–31.8‰ at 8.25 mbsf) exhibits the most depleted ^{13}C pool (Figs. F2, F3A), whereas Site 1062 (–20.2‰ at 66.60 mbsf) is least depleted in ^{13}C at the SMI (Fig. F3A). The mean value for $\delta^{13}C$ ΣCO_2 at the SMI is –26.2 ± 5‰; the median value is –28.5‰. Sites in order of increasing ^{13}C depletion at the SMI are 1062, 1054, 1055, 1063, 1060, 1061, and 1058/1059.

With increasing depth into the methanogenic zone, ΣCO_2 generally becomes progressively enriched in ^{13}C. Maximum ^{13}C enrichment occurs at Site 1054 (+12.2‰ at 195.70 mbsf) and minimum ^{13}C enrichment occurs at Site 1063 (–2.6‰ at 234.10 mbsf). The mean value of maximum ^{13}C enrichment for $\delta^{13}C$ ΣCO_2 is +4.3 ± 4.8‰; the median value is +3.3‰. The sites in order of increasing ^{13}C enrichment are 1063, 1062, 1060, 1061, 1055, 1058/1059, and 1054. The $\delta^{13}C$ values of ΣCO_2 at Sites 1061 (+3.3‰, 226 mbsf) and 1063 (–2.6‰, 234 mbsf) reach maximum values at ~171 and 215 m into the methanogenic zone, respectively, and then move toward increasing ^{13}C depletion with depth.

Methane

Methane $\delta^{13}C$ values of samples collected from sediment voids range from –65.8 (Site 1054; 197.16 mbsf) to –91.4‰ (Site 1063; 100.66 mbsf) (Table T2; Fig. F3B). The mean and median $\delta^{13}C$ values are –78.1 ± 6.2‰ and –79‰, respectively.

The carbon isotopic composition of methane is most depleted in ^{13}C nearest the SMI. Most methane samples are from sediment voids within core liners created by methane degassing during core recovery. Only when methane concentrations reach threshold levels are such gas-filled sediment voids available for sampling. However, at Site 1058/1059, six gas samples were collected in the uppermost methanogenic zone using

T1. Concentration and isotopic data of interstitial constituents from Leg 172 sites, p. 13.

T2. Carbon isotopic composition of interstitial methane and CO_2 gas at Leg 172 sites, p. 16.

F2. Pore-water concentration and carbon isotopic composition profiles, p. 11.

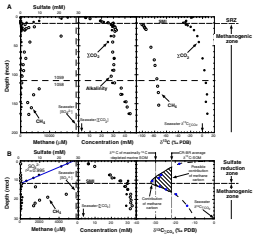

F3. Carbon isotopic values of interstitial dissolved CO_2 and methane plotted relative to the SMI, p. 12.

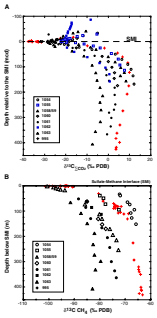

Reeburgh squeezers. The topmost sample has a $\delta^{13}C$ value of –100.6‰, almost 15‰ more depleted than the first sediment void sample at Site 1058/1059, and ~9‰ more depleted than the most negative $\delta^{13}C$ value of any other gas sample from Leg 172.

Methane becomes progressively enriched in ^{13}C with increasing depth below the SMI (Fig. F3B). Maximum ^{13}C enrichment occurs at Site 1054 (–65.8‰, 197 mbsf), whereas ^{13}C enrichment (–82.8‰, 416 mbsf) is at a minimum at Site 1063.

DISCUSSION

Anaerobic methane oxidation is a key process that controls the isotopic composition of ΣCO_2 and methane near the sulfate-methane interface. Cycling between these two carbon pools within an open system causes large ^{13}C depletions (Borowski et al., 1997). Because ΣCO_2 is so depleted in ^{13}C as it enters shallow methanogenic zone, when it serves as the substrate for CO_2 reduction the resultant methane is also strongly depleted in ^{13}C.

CO_2 reduction is the dominant methane-forming process within the shallow methanogenic zone of many marine deep-water localities (Whiticar et al., 1986), and the Blake Ridge region is no exception (e.g., Claypool and Kaplan, 1974; Claypool and Threlkeld, 1983; Galimov and Kvenvolden, 1983). Like other methane-rich regions, the carbon isotopic composition of each pool changes concomitantly with depth as ^{12}C is preferentially sequestered in methane. However, at some sites (1061 and 1063) the carbon isotopic composition of the pools begins to diverge with increasing depth as the ΣCO_2 pool becomes progressively enriched with ^{12}C.

Paull et al. (2000) suggest that lower rates of microbial methane production coupled with delivery of CO_2 and methane from below combine to cause this divergence in isotopic trends. Advection perhaps occurs at Leg 172 sites as well, although its effects are usually not observed, probably because of inadequate hole depths. At Sites 1061 and 1063 (the deepest holes), $\delta^{13}C$ ΣCO values become slowly but progressively lighter with increasing depth, moving toward typical $\delta^{13}C$ values of Blake Ridge sedimentary organic matter (–21‰; Borowski et al., 1998).

Data from ODP Leg 172 sites at the Blake-Bahama Ridge and Bermuda Rise are consistent with carbon isotopic data for ΣCO_2 and methane at other Blake Ridge sites (i.e., Sites 533, 994, 995, and 997; see references above) and at other continental margin sites worldwide (Borowski et al., 1997). The processes that create these isotopic trends are pervasive within the world's continental-rise sediments, although many factors combine to control the absolute carbon isotopic composition of ΣCO_2 and methane.

CONCLUSION

The dissolved carbon dioxide and methane pools within marine, continental-rise pore waters are geochemically coupled to one another through anaerobic methane oxidation and CO_2 reduction. In methane-rich settings, these processes cause consistent trends in isotopic composition that show: (1) maximum depletion of ^{13}C of the both pools near

the sulfate-methane interface; and (2) increasing proportions of ^{13}C in the ΣCO_2 pool with increasing depth in the shallow methanogenic zone. At locations with sufficiently deep holes, $\delta^{13}C$ values of ΣCO_2 may become more enriched in ^{12}C with increasing depth, moving in the direction of the carbon isotopic composition of sedimentary organic matter.

ACKNOWLEDGMENTS

We thank Neal Blair at North Carolina State University for his expertise in measuring dissolved CO_2 concentrations and CO_2 carbon isotopic composition. Chris Martens generously donated his facilities at the University of North Carolina at Chapel Hill, and Howard Mendlovitz made the isotopic measurements of CO_2 gas and methane. Anne Pimmel and Tim Bronk were indispensable in the chemistry lab aboard the *Resolution*, and our sampling could not been done without the rest of the *Resolution*'s marine laboratory technicians. JOI-USSSP provided the funds for shore-based isotopic measurements.

REFERENCES

Borowski, W.S., 1998. Pore-water sulfate concentration gradients, isotopic compositions, and diagenetic processes overlying continental margin, methane-rich sediments associated with gas hydrates. [Ph.D. dissert.]. Univ. of North Carolina, Chapel Hill, NC.

Borowski, W.S., Hoehler, T.M., Alperin, M.J., Rodriguez, N.M., and Paull, C.K., 2000. Significance of anaerobic methane oxidation in methane-rich sediments overlying the Blake Ridge gas hydrates. *In* Paull, C.K., Matsumoto, R., Wallace, P.J., and Dillon, W.P. (Eds.), *Proc. ODP, Sci. Results,* 164: College Station, TX (Ocean Drilling Program), 87–99.

Borowski, W.S., Paull, C.K., and Ussler, W., III, 1996. Marine pore-water sulfate profiles indicate in situ methane flux from underlying gas hydrate. *Geology,* 24:655–658.

————, 1997. Carbon cycling within the upper methanogenic zone of continental rise sediments: an example from the methane-rich sediments overlying the Blake Ridge gas hydrate deposits. *Mar. Chem.,* 57:299–311.

Claypool, G.E., and Kaplan, I.R., 1974. The origin and distribution of methane in marine sediments. *In* Kaplan, I.R. (Ed.), *Natural Gases in Marine Sediments:* New York (Plenum), 99–139.

Claypool, G.E., and Threlkeld, C.N., 1983. Anoxic diagenesis and methane generation in sediments of the Blake Outer Ridge, Deep Sea Drilling Project Site 533, Leg 76. *In* Sheridan, R.E., Gradstein, F.M., et al., *Init. Repts. DSDP,* 76: Washington (U.S. Govt. Printing Office), 391–402.

Craig, H., 1953. The geochemistry of the stable carbon isotopes. *Geochim. Cosmochim. Acta,* 3:53–92.

Deines, P., 1980. The isotopic composition of reduced organic carbon. *In* Fritz, P., and Fontes, J.C. (Eds.), *Handbook of Environmental Isotope Geochemistry* (Vol. 1)*: The Terrestrial Environment, A:* Amsterdam (Elsevier), 329–406.

Dillon, W.P., and Paull, C.K., 1983. Marine gas hydrates, II. Geophysical evidence. *In* Cox, J.L. (Ed.), *Natural Gas Hydrates: Properties, Occurrences, and Recovery:* Woburn, MA (Butterworth), 73–90.

Galimov, E.M., and Kvenvolden, K.A., 1983. Concentrations of carbon isotopic compositions of CH_4 and CO_2 in gas from sediments of the Blake Outer Ridge, Deep Sea Drilling Project Leg 76. *In* Sheridan R.E., Gradstein, F.M., et al., *Init. Repts. DSDP,* 76: Washington (U.S. Govt. Printing Office), 403–407.

Gieskes, J.M., 1981. Deep-sea drilling interstitial water studies: implications for chemical alteration of the oceanic crust, layers I and II. *In* Warme, J.E., Douglas, R.G., and Winterer, E.L. (Eds.), *The Deep Sea Drilling Project: A Decade of Progress*. Spec. Publ.—Soc. Econ. Paleontol. Mineral., 32:149–167.

Gieskes, J.M., Gamo, T., and Brumsack, H., 1991. Chemical methods for interstitial water analysis aboard *JOIDES Resolution. ODP Tech. Note,* 15.

Hoehler, T.M., Borowski, W.S., Alperin, M.J., Rodriguez, N.M., and Paull, C.K., 2000. Model, stable isotope, and radiotracer characterization of anaerobic methane oxidation in gas hydrate–bearing sediments of the Blake Ridge. *In* Paull, C.K., Matsumoto, R., Wallace, P.J., and Dillon, W.P. (Eds.), *Proc. ODP, Sci. Results,* 164: College Station, TX (Ocean Drilling Program), 79–85.

Hollister, C.D., Ewing, J.I., et al., 1972. *Init. Repts. DSDP,* 11: Washington (U.S. Govt. Printing Office).

Keigwin, L.D., Rio, D., Acton, G.D., et al., 1998. *Proc. ODP, Init. Repts.,* 172: College Station, TX (Ocean Drilling Program).

Kvenvolden, K.A., and McDonald, T.J., 1985. Gas hydrates of the Middle America Trench—Deep Sea Drilling Project Leg 84. *In* von Huene, R., Aubouin, J., et al., *Init. Repts. DSDP,* 84: Washington (U.S. Govt. Printing Office), 667–682.

Manheim, F.T., 1966. A hydraulic squeezer for obtaining interstitial waters from consolidated and unconsolidated sediments. *Geol. Surv. Prof. Pap. U.S.,* 550-C:256–261.

Manheim, F.T., and Sayles, F.L., 1974. Composition and origin of interstitial waters of marine sediments, based on deep sea drill cores. *In* Goldberg, E.D. (Ed.), *The Sea* (Vol. 5): *Marine Chemistry: The Sedimentary Cycle:* New York (Wiley), 527–568.

Martens, C.S., and Berner, R.A., 1974. Methane production in the interstitial waters of sulfate-depleted marine sediments. *Science,* 185:1167–1169.

Merritt, D.A., and Hayes, J.M., 1995. Carbon isotopic analysis of atmospheric methane by isotope-ratio-monitoring gas chromatography-mass spectrometry. *J.Geophys. Res.,* 100:1317–1326.

Paull, C.K., Lorenson, T.D., Borowski, W.S., Ussler, III, W., Olsen, K., and Rodriguez, N.M., 2000. Isotopic composition of CH_4, CO_2 species, and sedimentary organic matter within samples from the Blake Ridge: gas source implications. *In* Paull, C.K., Matsumoto, R., Wallace, P.J., and Dillon, W.P. (Eds.), *Proc. ODP, Sci. Results,* 164: College Station, TX (Ocean Drilling Program), 67–78.

Paull, C.K., Matsumoto, R., Wallace, P.J., et al., 1996. *Proc. ODP, Init. Repts.,* 164: College Station, TX (Ocean Drilling Program).

Popp, B.N., Sansone, F., Francis, F.J., and Rust, T.M., 1995. Determination of concentration and carbon isotopic composition of dissolved methane in sediments and nearshore waters. *Anal. Chem.,* 67:405–411.

Reeburgh, W.S., 1967. An improved interstitial water sampler. *Limnol. Oceanogr.,* 12:163–165.

————, 1976. Methane consumption in Cariaco Trench waters and sediments. *Earth Planet. Sci. Lett.,* 28:337–344.

Richards, F.A., 1965. Anoxic basins and fjords. *In* Riley, J.P., and Skirrow, G. (Eds.), *Chemical Oceanography* (Vol. 1): New York (Academic Press), 611–645.

Rodriguez, N.M., Paull, C.K., and Borowski, W.S., 2000. Zonation of authigenic carbonates within gas hydrate–bearing sedimentary sections on the Blake Ridge: offshore southeastern North America. *In* Paull, C.K., Matsumoto, R., Wallace, P.J., and Dillon, W.P. (Eds.), *Proc. ODP, Sci. Results,* 164: College Station, TX (Ocean Drilling Program), 301–312.

Sheridan, R.E., Gradstein, F.M., et al., 1983. *Init. Repts. DSDP,* 76: Washington (U.S. Govt. Printing Office).

Whiticar, M.J., Faber, E., and Schoell, M., 1986. Biogenic methane formation in marine and freshwater environments: CO_2 reduction vs. acetate fermentation—isotope evidence. *Geochim. Cosmochim. Acta,* 50:693–709.

Figure F1. Map showing the location of DSDP and ODP sites at the Carolina Rise, Blake Ridge, and Bahama Ridge. DSDP Leg 11 Sites 102, 103, and 104 (Hollister, Ewing, et al., 1972) and DSDP Leg 76 Site 533 (Sheridan, Gradstein, et al., 1983) are shown with triangles. ODP Leg 164 sites are shown with circles; Sites 994, 995, and 997 (Paull, Matsumoto, Wallace, et al., 1996) have relevance to this study. ODP Leg 172 sites, noted by diamonds, include those on the Carolina Rise (1054–1057), on the Blake Ridge (1058–1061), and on the Bahama Ridge (1062) (Keigwin, Rio, Acton, et al., 1998). Site 1063 is not plotted on the map but is located ~850 nmi east-northeast of the Blake Ridge on the northeast Bermuda Rise. The stippled areas encompass the region where bottom-simulating reflectors (BSRs) occur, indicative of the presence of gas hydrates within the sediments (Dillon and Paull, 1983).

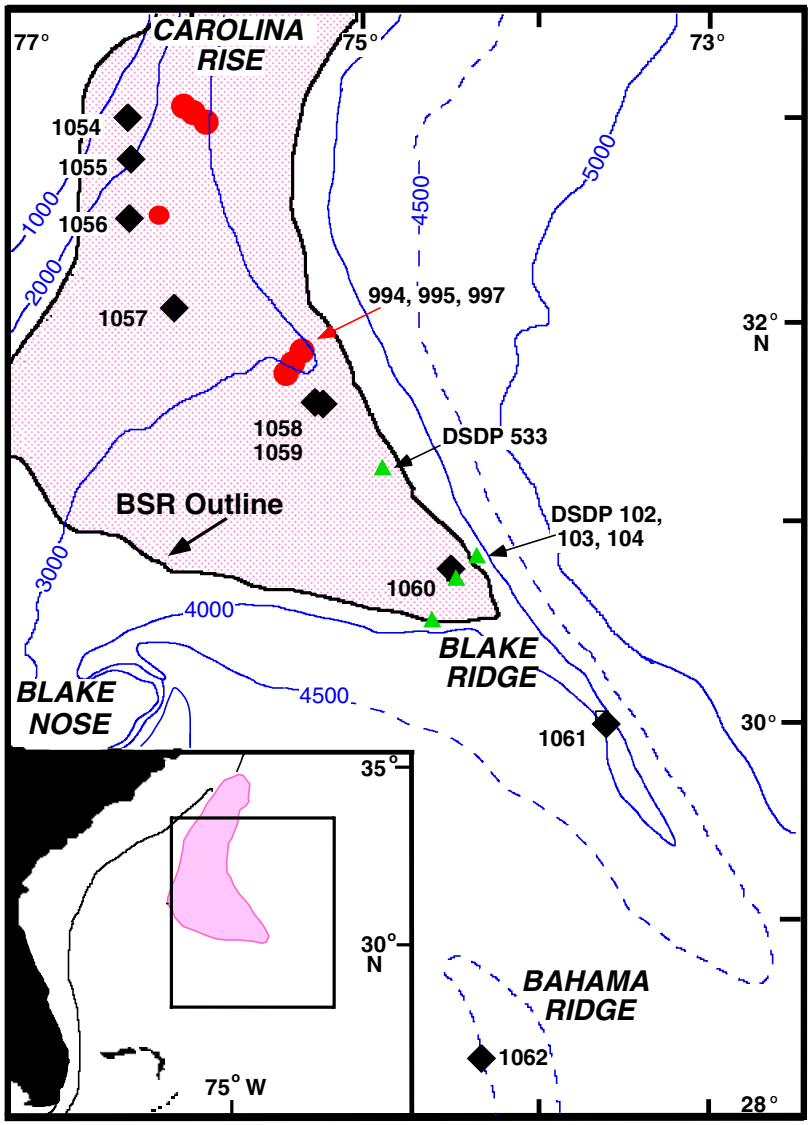

Figure F2. Pore water concentration and carbon isotopic composition profiles at Leg 172 Sites 1058 and 1059, plotted as a single hole location (separated laterally by ~4 nmi). Depth is plotted as meters corrected depth (mcd) below the sediment-water interface (see Keigwin, Rio, Acton, et al., 1998, for explanation). Data above 114.31 mcd (96.15 mbsf) are from Site 1059; data below this depth are from Site 1058. **A.** The entire sampled sediment column including the sulfate reduction zone (SRZ) and methanogenic zone. **B.** The upper 30 m of the sediment column showing profiles near the methane-sulfate interface (SMI). Sulfate, methane, ΣCO_2, and alkalinity values are reported in Table **T1.** Methane concentration is reported as micromolar units (µM)(Keigwin, Rio, Acton, et al., 1998); other concentration units are millimolar (mM). Carbon isotopic values are reported in per mil units (‰, relative to the Peedee belemnite [PDB] standard). ΣCO_2 isotopic values are tabulated in Table **T1;** methane isotopic values appear in Table **T2.** In the shallow $\delta^{13}C_{\Sigma CO2}$ profile, the shaded portion of the profile illustrates methane carbon in the CO_2 pool likely derived from methane through anaerobic methane oxidation, because marine sedimentary organic matter (SOM) is typically more ^{13}C-enriched than –30‰ PDB (Deines, 1980). The hatched portion of the curve shows carbon likely derived from methane because the isotopic composition of average SOM in sediments of the Carolina Rise and Blake Ridge is –21‰ (e.g., Borowski, 1998). The lower boundary of the curve is defined by a data point (–8.4‰, 33.45 mcd) that is not shown.

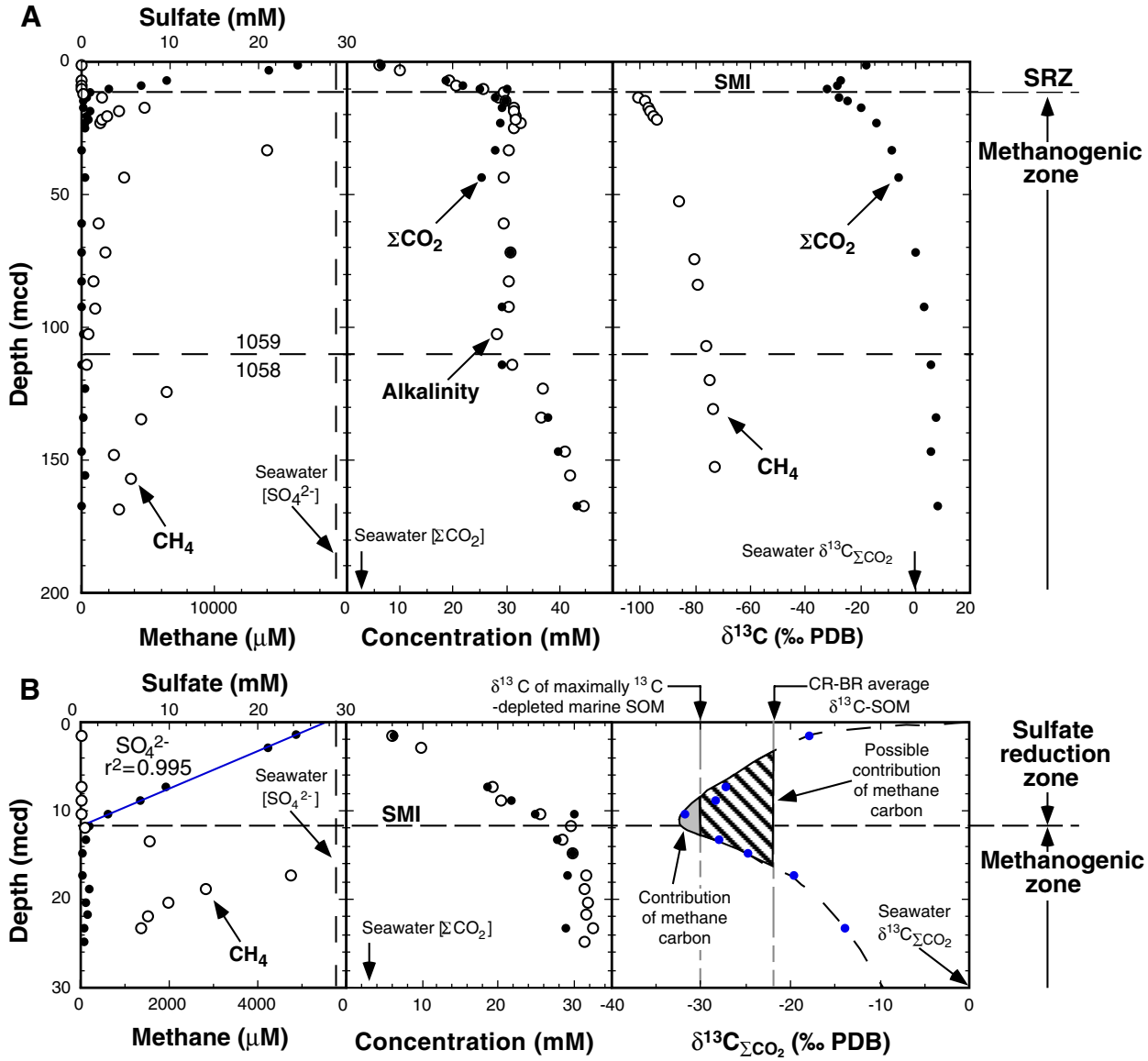

Figure F3. (**A**) Carbon isotopic values of interstitial dissolved CO_2 and (**B**) methane plotted as a function below the seabed in meters (meters corrected depth, mcd; see Keigwin, Rio, Acton, et al., 1998) relative to the sulfate-methane interface (SMI). ΣCO_2 isotopic values are tabulated in Table T1; methane isotopic values appear in Table T2. Site 995 data (ODP Leg 164) for ΣCO_2 and methane are from Borowski et al. (2000) and Paull et al. (2000), respectively.

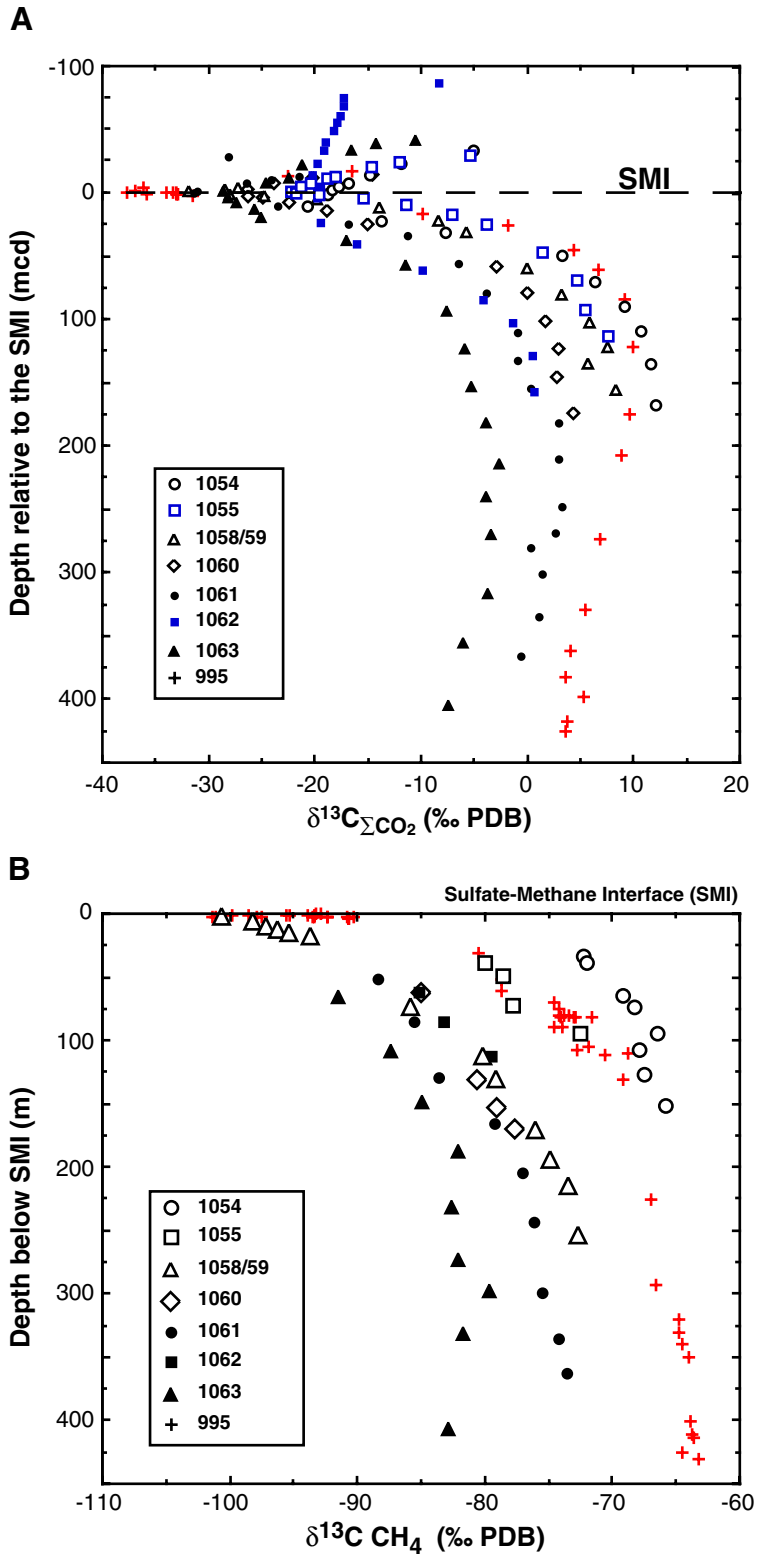

Table T1. Concentration and isotopic data of selected interstitial constituents from Leg 172 sites. (See table notes. Continued on next two pages.)

Core, section, interval (cm)	Depth (mbsf)	Depth (mcd)	Sulfate (mM)*	Alkalinity (mM)*	ΣCO_2 (mM)	$\delta^{13}C$ ΣCO_2 (‰ PDB)
172-1054A-						
1H-1, 145-150	1.45	1.45	27.6	4.6	4.8	–5.101
1H-5, 145-150	7.45	7.45	27.4	4.3	—	—
2H-3, 145-150	12.45	12.10	24.2	8.0	8.2	–11.844
3H-1, 145-150	18.95	20.20	21.0	10.9	11.4	–14.732
3H-6, 145-150	26.45	27.70	16.9	16.2	14.6	–16.794
4H-1, 145-150	28.45	29.35	13.0	19.4	16.6	–17.656
4H-3, 145-150	31.45	32.35	12.1	21.8	19.2	–18.338
4H-6, 145-150	35.95	36.85	10.3	23.8	20.2	–18.742
5H-5, 145-150	43.95	45.70	3.4	28.7	26.0	–20.711
6H-4, 140-150	54.90	56.75	0.0	33.5	31.9	–13.71
8H-1, 140-150	63.80	66.40	0.1	37.7	34.9	–7.683
10H-5, 140-150	82.70	84.45	0.2	43.1	46.7	3.3
12X-4, 140-150	99.40	105.49	0.1	50.7	57.1	6.4
14X-4, 140-150	118.60	124.59	0.0	55.8	62.1	9.2
16X-2, 135-150	137.75	143.74	0.6	56.9	63.4	10.7
19X-2, 140-150	163.80	169.79	0.5	65.2	65.0	11.6
22X-4, 140-150	195.70	201.69	0.2	67.8	67.6	12.2
172-1055B-						
1H-1, 145-150	1.45	1.60	27.4	3.9	4.4	–5.437
2H-1, 145-150	5.95	5.90	25.3	6.6	7.0	–11.991
2H-4, 145-150	10.45	10.40	21.1	9.0	9.2	–14.593
3H-1, 145-150	15.45	18.58	11.9	13.9	13.7	–18.036
3H-2, 145-150	16.95	20.08	9.9	16.4	14.8	–18.742
3H-4, 145-150	19.95	23.08	7.1	17.9	16.4	–20.401
3H-6, 145-150	22.95	26.08	4.0	19.6	17.6	–21.359
4H-1, 145-150	24.95	29.38	0.5	21.8	19.3	–22.287
4H-2, 145-150	26.45	30.88	0.3	21.0	18.3	–21.73
4H-3, 145-150	27.95	32.38	0.1	21.2	19.5	–19.592
4H-5, 145-150	30.95	35.38	0.0	20.4	18.4	–15.396
5H-1, 145-150	34.40	40.12	0.1	21.2	20.3	–11.445
5H-6, 140-150	41.90	47.62	0.1	23.1	21.5	–7.115
6H-5, 140-150	49.90	56.32	0.4	24.8	23.4	–3.834
8H-6, 140-150	70.40	78.21	0.1	31.6	30.7	1.4
10H-6, 140-150	89.40	99.86	0.6	38.7	34.7	4.7
12H-6, 140-150	108.13	122.62	0.4	41.0	43.2	5.5
14H-6, 135-150	126.43	144.16	0.2	48.5	48.4	7.7
172-1058A-						
2H-5, 140-150	16.90	19.35	0.2	28.2	29.1	—
13H-5, 140-150	120.65	134.02	0.2	36.4	37.7	7.6
14H-7, 140-150	132.80	146.79	0.0	40.9	39.7	5.8
16H-5, 140-150	148.66	167.14	0.0	44.6	43.4	8.3
172-1059A-						
1H-1, 145-150	1.45	1.45	24.5	6.1	6.4	–17.828
2H-1, 145-150	5.25	7.32	9.6	19.4	18.5	–27.204
2H-2, 145-150	6.75	8.82	6.7	20.5	21.7	–28.361
2H-3, 145-150	8.25	10.32	3.2	25.6	25.0	–31.806
2H-5, 145-150	11.25	13.32	0.5	28.6	27.8	–27.954
2H-6, 145-150	12.75	14.82	0.2	29.8	29.8	–24.668
3H-1, 145-150	14.75	17.30	0.2	31.5	29.2	–19.712
3H-5, 145-150	20.75	23.30	0.5	32.5	29.0	–13.871
4H-6, 62-72	30.42	33.45	0.0	30.6	27.8	–8.36
5H-5, 150-160	39.80	43.36	0.5	29.6	25.5	–5.727
7H-6, 140-150	60.20	71.84	0.0	30.7	30.8	0.0
9H-5, 140-150	77.70	92.56	0.0	30.6	29.3	3.2
11H-5, 140-150	96.15	114.31	0.1	31.2	29.1	5.9
172-1060A-						
1H-1, 145-150	1.45	1.45	25.3	6.2	5.4	–16.097
1H-3, 145-150	4.45	4.45	18.6	12.8	9.7	–21.776
1H-5, 145-150	7.45	7.45	12.2	17.5	16.1	–25.28
2H-1, 145-150	10.45	12.39	3.5	—	22.3	–27.824
2H-2, 145-150	11.95	13.89	1.3	26.9	—	—
2H-3, 145-150	13.45	15.39	0.8	28.2	—	—
2H-4, 145-150	14.95	16.89	0.2	26.2	29.1	–28.926
2H-5, 145-150	16.45	18.39	0.1	25.6	27.6	–27.818

Table T1 (continued).

Core, section, interval (cm)	Depth (mbsf)	Depth (mcd)	Sulfate (mM)*	Alkalinity (mM)*	ΣCO_2 (mM)	$\delta^{13}C$ ΣCO_2 (‰ PDB)
2H-6, 145-150	17.95	19.89	0.7	28.6	27.2	–26.368
3H-1, 140-150	19.90	23.90	0.1	28.6	26.7	–23.961
3H-5, 140-150	25.90	29.90	0.1	27.2	—	–20.355
4H-5, 146-156	35.46	40.08	0.2	23.6	23.5	–16.421
5H-5, 144-154	44.94	50.81	—	—	22.7	–10.633
7H-5, 140-150	63.90	74.29	0.0	24.3	21.2	–4.382
9H-5, 140-150	82.90	95.06	0.0	21.7	19.5	–1.534
11H-5, 140-150	101.90	117.09	0.0	19.3	16.5	0.2
13H-5, 140-150	119.40	138.23	0.0	19.3	16.8	1.4
15H-5, 140-150	139.90	160.53	0.2	16.7	14.4	1.4
18H-5, 140-150	168.10	188.73	0.3	15.2	14.0	2.8
172-1061A-						
2H-4, 140-150	15.40	28.49	0.0	26.2	24.9	–23.449
3H-5, 146-150	26.46	42.29	0.0	22.6	20.1	–16.824
4H-5, 140-150	35.90	52.35	0.0	23.3	21.5	–11.162
6H-5, 145-150	54.90	74.25	0.0	22.0	20.2	–6.493
8H-5, 145-150	73.76	96.81	0.2	20.0	17.6	–3.776
11H-5, 140-150	102.40	128.69	0.0	17.3	15.4	–0.905
13H-5, 140-150	121.40	150.74	0.0	14.9	10.1	–0.819
15H-5, 140-150	140.40	173.12	0.0	13.1	11.5	0.4
18X-4, 135-150	162.76	200.28	0.6	13.3	11.3	3.0
21X-3, 135-150	189.60	228.87	0.0	13.1	11.5	3.0
25X-1, 125-150	226.05	265.32	0.0	10.8	8.4	3.3
27X-3, 125-150	247.53	286.80	0.0	9.3	7.9	2.6
28X-4, 100-125	258.66	297.93	0.0	6.1	5.7	0.3
30X-5, 125-150	279.92	319.19	0.0	5.7	5.3	1.4
34X-1, 120-150	312.90	352.17	0.0	6.1	5.1	1.1
37X-3, 120-150	344.70	383.97	0.1	6.5	5.5	–0.594
172-0161E-						
1H-1, 145-150	1.45	1.45	25.2	—	6.2	–14.83
1H-2, 145-150	2.95	2.95	—	—	9.7	–19.167
1H-4, 145-150	5.35	5.35	18.2	12.1	11.2	–21.429
1H-6, 145-150	8.35	8.35	12.2	17.6	14.6	–24.003
2H-1, 145-150	10.85	10.85	8.2	21.5	18.1	–26.346
2H-3, 145-150	13.85	13.85	5.0	25.2	21.3	–28.059
2H-5, 132-137	16.72	16.72	1.1	26.8	25.4	–30.978
2H-6, 145-150	18.22	18.22	0.5	28.2	25.8	–31.293
172-1062A-						
1H-1, 145-150	1.45	1.45	27.5	4.8	5.0	–8.363
2H-1, 140-150	3.60	6.00	22.3	9.1	1.3	
2H-2, 140-150	5.10	7.50	—	—	—	–15.089
2H-4, 140-150	8.10	10.50	—	—	—	–16.099
2H-6, 140-150	11.10	13.50	17.2	13.9	12.3	–17.241
3H-3, 140-150	16.10	19.02	14.0	15.6	15.3	–17.279
4H-1, 140-150	22.60	27.04	10.5	17.6	16.6	–17.632
4H-5, 140-150	28.60	33.04	8.6	19.2	19.1	–17.936
5H-2, 140-150	33.60	38.40	6.8	—	18.9	–18.269
6H-1, 140-150	41.60	48.62	4.2	21.2	17.4	–18.972
6H-5, 140-150	47.60	54.62	3.5	19.6	19.2	–19.094
7H-5, 140-150	57.10	65.14	1.4	18.8	16.6	–19.729
8H-5, 140-150	66.60	74.26	0.5	18.5	17.4	–20.211
9H-5, 140-150	76.10	83.10	0.2	16.2	16.2	–19.452
10H-5, 140-150	85.60	92.46	0.3	14.9	12.8	–19.796
12H-4, 140-150	103.10	111.00	0.0	12.6	10.6	–19.373
14H-3, 135-150	120.55	128.91	0.0	8.7	7.2	–15.96
16H-4, 135-150	140.65	149.67	0.0	7.6	6.8	–9.863
18H-4, 135-150	160.05	171.99	0.3	8.3	7.7	–4.066
20H-4, 135-150	179.05	190.99	0.2	10.6	7.6	–1.326
172-1062B-						
23X-5, 140-150	216.86	216.86	0.0	10.9	10.0	0.5
26X-5, 125-150	245.61	245.61	0.2	12.6	12.6	0.7
172-1063A-						
1H-1, 140-150	1.40	1.40	25.9	4.5	5.3	–10.46
1H-3, 140-150	4.40	4.40	22.3	—	8.8	–14.178
2H-3, 140-150	8.52	9.38	14.4	14.8	15.5	–16.427
3H-3, 140-150	19.20	20.88	4.5	24.1	22.4	–21.106
3H-6, 140-150	23.70	23.70	—	—	23.7	–19.654
4H-3, 140-150	28.70	30.56	3.6	22.8	20.4	–22.379
4H-6, 140-150	33.20	35.06	2.3	22.3	20.4	–24.611

Table T1 (continued).

Core, section, interval (cm)	Depth (mbsf)	Depth (mcd)	Sulfate (mM)*	Alkalinity (mM)*	ΣCO_2 (mM)	$\delta^{13}C$ ΣCO_2 (‰ PDB)
5H-3, 140-150	38.20	41.64	0.1	23.6	21.2	–28.51
5H-6, 140-150	42.70	46.14	—	23.4	20.8	–28.041
6H-3, 140-150	47.70	51.22	0.5	22.5	20.9	–27.265
6H-6, 140-150	52.20	55.72	0.2	22.0	17.7	–25.642
7H-3, 140-150	57.20	61.66	0.5	19.2	18.5	–24.952
9H-3, 140-150	76.20	80.76	0.2	17.1	14.9	–16.954
11H-5, 140-150	98.20	104.76	0.0	15.0	13.8	–11.325
14H-5, 135-150	126.04	136.42	0.3	11.6	9.9	–7.496
17H-5, 135-150	154.25	166.19	0.0	10.1	9.2	–5.871
20H-5, 139-159	183.23	196.28	0.0	8.8	7.7	–5.214
23X-4, 130-150	207.20	224.43	0.7	6.7	5.8	–3.738
26X-5, 130-150	234.10	256.39	0.0	5.3	4.6	–2.569
29X-3, 130-150	259.60	283.05	0.7	3.1	2.4	–3.88
32X-3, 117-142	288.27	312.29	0.5	5.4	4.8	–3.424
36X-5, 125-150	326.85	358.74	0.0	4.5	3.7	–3.625
40X-4, 125-150	366.45	398.34	0.4	2.4	1.7	–5.93
45X-5, 120-150	415.95	447.84	0.2	3.7	3.9	–7.39

Notes: mbsf = meters below seafloor, mcd = meters corrected depth. mM = millimoles per liter or millimolar. Isotopic values in per mil (‰) relative to the Peedee belemnite (PDB) standard. * = shipboard determinations (Keigwin, Rio, Acton, et al., 1998).

Table T2. Carbon isotopic composition of interstitial methane and CO_2 gas at Leg 172 sites.

Core, section	Depth (mbsf)	Depth (mcd)	$\delta^{13}C$ CH_4 (‰ PDB)	$\delta^{13}C$ CO_2 gas (‰ PDB)
172-1054A-				
6H-5	52.51	54.36	—	—
10H-6	84.16	85.91	–72.23	—
11X-3	89.16	91.21	–72	—
13X-5	110.36	116.35	–69.21	—
14X-5	119.22	125.21	–68.28	0.9
16X-6	140.76	146.75	–66.49	0.1
18X-2	154.06	160.05	–67.83	2.3
20X-2	173.36	179.35	–67.41	3.8
22X-5	197.16	203.15	–65.75	2.0
172-1055B-				
8H-1	61.50	69.31	–79.95	—
9H-1	71.00	79.51	–78.5	—
11H-2	90.00	102.07	–77.83	–3.42
13H-3	109.00	124.60	–72.54	—
172-1058A-				
8H-1	67.60	74.29	–80.15	—
9H-1	76.43	84.10	–79.03	—
11H-2	97.00	106.78	–76.02	—
12H-3	107.58	119.67	–74.78	—
13H-3	117.56	130.93	–73.46	—
15H-3	136.15	152.42	–72.68	—
172-1059A-				
2H-5*	11.25	13.32	–100.6	–30.53
2H-6*	12.75	14.82	–98.2	–26.19
3H-1*	14.75	17.30	–97.14	–22.64
3H-2*	16.25	18.80	–96.16	–19.17
3H-3*	17.75	20.30	–95.27	–21.66
3H-4*	19.25	21.80	–93.62	–20.54
6H-1	42.47	52.47	–85.76	—
172-1060A-				
8H-2	67.57	79.64	–84.99	—
11H-1	95.98	111.17	–77.38	—
14H-3	126.82	147.45	–80.58	—
16H-5	145.58	169.44	–79.11	—
18H-4	166.65	187.28	–77.68	—
172-1061A-				
6H-1	48.91	68.26	–88.3	–4.4
9H-1	77.03	102.08	–85.56	—
13H-3	117.15	146.49	–83.62	—
16H-5	147.44	182.56	–79.22	—
20X-4	182.07	221.34	–76.97	—
24X-4	220.91	260.18	–76.15	—
30X-4	277.67	316.94	–75.52	—
34X-2	313.68	352.95	–74.2	—
37X-1	341.07	380.34	–73.56	—
172-1062A-				
16H-1	136.28	145.30	–85.08	—
18H-3	157.27	169.21	–83.18	—
21X-4	187.08	196.04	–79.42	—
172-1063A-				
12H-1	100.66	107.66	–91.38	—
16H-1	139.25	150.53	–87.36	—
20H-1	177.48	190.53	–84.81	—
24X-2	209.69	228.92	–82.07	—
28X-3	250.18	273.63	–82.52	—
32X-2	291.46	315.48	–82.02	—
34X-6	312.11	339.28	–79.53	—
38X-1	341.92	373.81	–81.6	—
45X-6	416.32	448.21	–82.81	—

Notes: mbsf = meters below seafloor, mcd = meters corrected depth. Isotopic values in per mil (‰) relative to the Peedee belemnite (PDB) standard. * = Reeburgh squeezer samples.